High-spin structures and alignment properties in ^{126}Ce

A. N. Wilson[*] and R. Wadsworth
Department of Physics, University of York, Heslington Y010 5DD, United Kingdom

J. F. Smith, S. J. Freeman, and M. J. Leddy
Schuster Laboratory, University of Manchester, Manchester MP13 9PL, United Kingdom

C. J. Chiara, D. B. Fossan, D. R. LaFosse, and K. Starosta[†]
Department of Physics and Astronomy, State University of New York at Stony Brook, Stony Brook, New York 11794-3800

M. Devlin, D. G. Sarantites, and J. N. Wilson
Department of Chemistry, Washington University, St. Louis, Missouri 63130

M. P. Carpenter, C. N. Davids, R. V. F. Janssens, and D. Seweryniak
Argonne National Laboratory, Argonne, Illinois 60439

R. Wyss
KTH, Royal Institute of Technology, Frescativägen 24, S-104 05 Stockholm, Sweden

Excited states in ^{126}Ce have been observed with the GAMMASPHERE γ-ray detector array, used in conjunction with the MICROBALL charged-particle detector. The reaction ^{64}Zn(^{64}Zn, $xpn\alpha$) (beam energy 260 MeV) was used to populate a wide range of nuclei in the neutron-deficient region with $A \approx 120$. ^{126}Ce was populated via the $2p$ evaporation channel. The three previously observed bands have been extended to higher spins and some other structures have been identified. The yrast band shows evidence of a delayed neutron alignment occurring at a rotational frequency $\omega \approx 0.5$ MeV/$\hbar$ as observed in the neighboring odd-A nucleus ^{127}Pr. One of the two excited bands shows evidence for a similar crossing at a slightly lower frequency and also exhibits a sudden gain in alignment at $\omega = 0.57$ MeV/$\hbar$. The third band may involve the coupling of a γ-vibrational state. All three rotational bands are discussed in terms of standard and extended cranked shell model calculations.

I. INTRODUCTION

Neutron-deficient nuclei with $50 \leq Z \leq 60$ provide an important means of testing the underlying assumptions of the standard cranked shell model (CSM). Lighter nuclei with $N \approx Z$ exhibit structures that suggest that the pairing force between neutrons and protons occupying the same orbitals has a strong influence on the behavior of the nucleus. In these heavier nuclei, the neutrons and protons both occupy high-j $h_{11/2}$ intruder orbitals; however, the neutron levels are filled up to the mid- to high-Ω orbitals, while the proton Fermi surface is lower in the shell. Thus these nuclei present a region in which the neutron-proton pairing effects are not expected to be so strong, but where the forces may be modified as compared to isotopes closer to stability. Indeed, strong evidence for the need to use extended CSM [1] calculations including a quadrupole-quadrupole pairing term has been observed in the nuclei ^{127}Pr and ^{131}Pm [2]. This

type of calculation [1] has proved extremely successful in describing superdeformed structures in the $A \approx 190$ region [3] and has also been applied to structures based on intruder states in nuclei with $A \approx 110$ [4]. In general, these calculations have found their most successful applications when applied to odd-A nuclei, as they allow the state of the odd particle to be blocked self-consistently. However, there are several other salient differences from ''standard'' CSM calculations that may imply that they are more suitable for use in describing these very neutron-deficient nuclei. Both pairing and deformation are determined self-consistently and the pairing interaction itself is modified to include a quadrupole as well as a monopole force. As will be discussed later, standard calculations do not generally provide accurate predictions of crossing frequencies and alignment gains in this very neutron-deficient mass region. While the extended calculations have proved satisfactory for describing the behavior of the ground-state band in ^{127}Pr, one wishes to see evidence of their applicability in other nuclei.

The yrast bands in the heavier ($A \approx 130$) Ce isotopes are characterized by the alignment of a pair of $h_{11/2}$ protons at spin $I \approx 10\hbar$ and rotational frequency $\omega \approx 0.3-0.4$ MeV/$\hbar$. This crossing is well reproduced by standard CSM calculations. However, the same calculations predict a second alignment of a pair of $h_{11/2}$ quasineutrons that is generally ob-

―――――
*Present address: Department of Nuclear Physics, Research School of Physical Sciences and Engineering, Australian National University, Canberra ACT 0200, Australia.

†On leave from Institute of Experimental Physics, Warsaw University, Hoza 69, 00-681 Warsaw, Poland.

served at a higher spin (and over a larger frequency range) than expected. Recent results concerning the nucleus ^{128}Ce [5] have been interpreted as being solely based on quasiproton excitations, explaining the second alignment gain in the ground-state band as being due to a second quasiproton alignment, rather than to the predicted $h_{11/2}$ neutrons. Clearly, the standard CSM calculations fail to reproduce the experimentally observed behavior. It is a matter of debate whether the neutron crossing is completely absent or whether, as the extended CSM calculations suggest, it occurs at a higher frequency than the standard model predicts. The frequency at which the first $h_{11/2}$ quasineutron alignment occurs is predicted to decrease with decreasing neutron number and, thus, one might expect to observe it in the yrast structures of the lighter Ce isotopes. The present data for the more neutron-deficient ^{126}Ce show a gradual gain in alignment around $\omega \approx 0.5$ MeV/$\hbar$ in addition to the earlier (sharper) proton crossing. This behavior is discussed in terms of both standard and extended CSM calculations.

In addition to the study of the yrast band, the two previously known [6] excited bands have been extended to higher spin and excitation energy. One of these bands (band 2) shows some evidence for the neutron alignment thought to be observed in band 1; in addition, there is a sharp rise in the aligned angular momentum at high frequency ($\omega = 0.57$ MeV/$\hbar$) that is not predicted by the standard calculations. This band was previously assigned as being of negative parity [6]; somewhat ambiguous indications of its parity are found in the current work, preventing a definite assignment from being made. The other band (band 3) is suggested to be of positive parity. This band clearly undergoes the $h_{11/2}$ proton alignment common to the yrast bands in the Ce isotopes, but subsequently displays no other evidence of any interaction. Comparisons with excited structures in nearby Ba nuclei support the assertion that this structure may involve a γ-vibrational state, coupled to the quasiparticle vacuum at low spin and to the S-band above the first band crossing.

II. EXPERIMENTAL DETAILS

The experiment was carried out at Argonne National Laboratory. The beam of ^{64}Zn, provided by the ATLAS accelerator at an energy of 260 MeV, was incident on a target consisting of two stacked, thin foils (each of thickness 500 μg cm^{-2}) of ^{64}Zn for a total period of approximately 56 h. Gamma rays emitted from recoiling nuclei were detected using the GAMMASPHERE array [7], which consisted of 101 Ge detectors, 66 of which (situated at angles close to 90° relative to the beam direction) were electronically segmented into two halves. The remaining detectors were mounted in rings at more backward and forward angles. The ring at 17.3° was left empty to allow for the opening angle of the Argonne Fragment Mass Analyzer (FMA) [8]; however, the M/q information provided by this device was not used in the analysis presented here. Charged particles (protons and α particles) emitted during the reaction were detected using the MICROBALL array [9] of CsI(Tl) detectors. Events were written to tape when a minimum of four γ rays were detected in prompt coincidence. The data recorded included γ-ray en-

ergies (gain matched to 1/3 keV per channel but with no Doppler correction applied), timing information, energies and times from the MICROBALL and position and timing information for recoils detected in the FMA.

III. ANALYSIS METHODS

In the ^{64}Zn + ^{64}Zn reaction, ^{126}Ce is produced after prompt evaporation of two protons only. The strongest reaction channel ($\alpha 2p$) led to the population of ^{122}Ba; ^{126}Ce was produced with approximately 30% of this intensity. In the off-line analysis, it was possible to minimize contamination from other channels by setting requirements on the particles detected in the MICROBALL in prompt coincidence with γ rays. Initially, the condition of exactly two protons and zero α particles was imposed in order to select out γ rays associated with the decay of ^{126}Ce. It was subsequently found that, because of less than 100% efficiency for the detection of charged particles, allowing 1p events to be included significantly increased the statistics for the channel of interest without introducing an excessive level of contamination from other reaction products. Excluding those events in which more than two protons or any α particles were detected was found to be essential in order to reduce the presence of stronger channels leading to lighter nuclei (isotopes of La, Ba etc) that would otherwise dominate the spectrum.

With the use of a thin target, γ rays emitted from the recoiling nuclei experience the full Doppler shift. The reaction used results in a high v/c (≈ 0.04) that is altered by the emission of particles as the compound nucleus decays to the final residues. This effect was compensated for by using the MICROBALL to perform event-by-event Doppler-shift corrections. The following sorting methods were then applied.

(i) Two three-dimensional histograms (cubes) were created in a format suitable for analysis with the RADWARE [10] package. Background subtraction was performed using the FUL method [11]. Each cube contained γ rays with energies between 80 keV and 2000 keV, which were binned so as to preserve a constant channel full-width half-maximum for the γ-ray peaks across the entire energy range. The first was created with the requirement that either one or two protons and no α particle were detected in the MICROBALL; this cube contained $\approx 1.3 \times 10^{10}$ triple γ coincidences. No particle detection requirements were applied to the second cube, which simply contained all γ rays within the required energy range. This cube contained $\approx 2.4 \times 10^{10}$ triple γ coincidences.

(ii) A series of one-dimensional coincidence spectra were produced with multiple gates set on various structures observed in the cubes (see Sec. IV). Due to the nonlinear gain applied to the γ rays incremented into the cubes, the energy dispersion at high E_γ reduces the precision with which centroids can be measured. The one-dimensional (1D) spectra were created using gains of 1/3- and 2/3-keV per channel, and subsequently allowed a more accurate measurement of the peak centroids. Background subtraction was achieved by subtracting normalized combinations of spectra sorted using the same lists of gates but lower gate folds. That is, for a

spectrum created requiring three gates from list A, the background spectrum was created by combining a spectrum of γ rays from events in which two gates from list A are satisfied, one of events in which one gate from list A has been satisfied and the total projection of the data.

(iii) The data were also sorted into γ-γ coincidence matrices with the aim of determining the multipolarity of γ-ray transitions in ^{126}Ce. Gamma rays detected at the forward/backward (FB) angles (i.e., $\theta \leq 38°$ or $\theta \geq 143°$ with respect to the beam direction) were incremented on one axis with coincident γ rays detected at angles of $79° \leq \theta \leq 101° (\sim 90°)$ on the other. Such matrices were created both with and without γ-ray coincidence gates in order to enhance structures of specific interest (see Sec. IV). In all cases, only events in which one or two protons (and zero α particles) had been detected in the MICROBALL were incremented. These asymmetric matrices were created in a format suitable for analysis with the UPAK [12] package. A background subtraction was performed on each of these matrices using the BAC-PAC software [13], which implements the Palameta-Waddington [14] method for asymmetric two-dimensional histograms. The experimental ratio

$$R_{DCO} = \frac{I_\gamma(\text{observed at } FB, \text{ gate on} \sim 90°)}{I_\gamma(\text{observed at} \sim 90°, \text{ gate on } FB)} \quad (1)$$

was then measured and the method of directional correlations from oriented states (DCO) [15] was used to interpret these data. The effect on this ratio of setting γ-ray gates before incrementing the matrices is minimal, as the gating transitions were allowed to be detected at any angle. This means that any extraneous correlation effects introduced by gating in the sort are negligible. Similarly, the isotropic construction of the MICROBALL implies that the use of particle gates should have no effect.

IV. RESULTS AND LEVEL SCHEME

The partial level scheme for ^{126}Ce deduced in this work is presented in Fig. 1, with the properties of the transitions given in Table I. The ground-state band (band 1) has been extended by the observation of eight more transitions, giving the spin and excitation energy of the highest observed level as $I^\pi = 36^+$, $E_{ex} = 16.020$ MeV. Eight more transitions have also been added to band 2 [previously observed to spin $I^\pi = (23^-)$], giving a maximum spin and excitation energy of $I^\pi = (39^-)$ and $E_{ex} = 16.602$ MeV. An 1185-keV transition has been observed to link the second level in band 2 to the 6^+ level in band 1. The structure previously reported as band 3 has been clarified and extended by nine transitions to a maximum observed spin of $I^\pi = 28^+$ (and excitation energy $E_{ex} = 10.873$ MeV). The 1016-keV γ ray observed by Morek *et al.* to feed the 6^+ level in band 1 has been confirmed, and another structure has been observed above this state. This γ ray has been found in this work to be in coincidence with members of band 3. Gated γ-ray spectra representative of the decay of the three bands are presented in Fig. 2. Figure 2(a) shows a background-subtracted, double-gated spectrum obtained by setting gates on all transitions in the ground-state
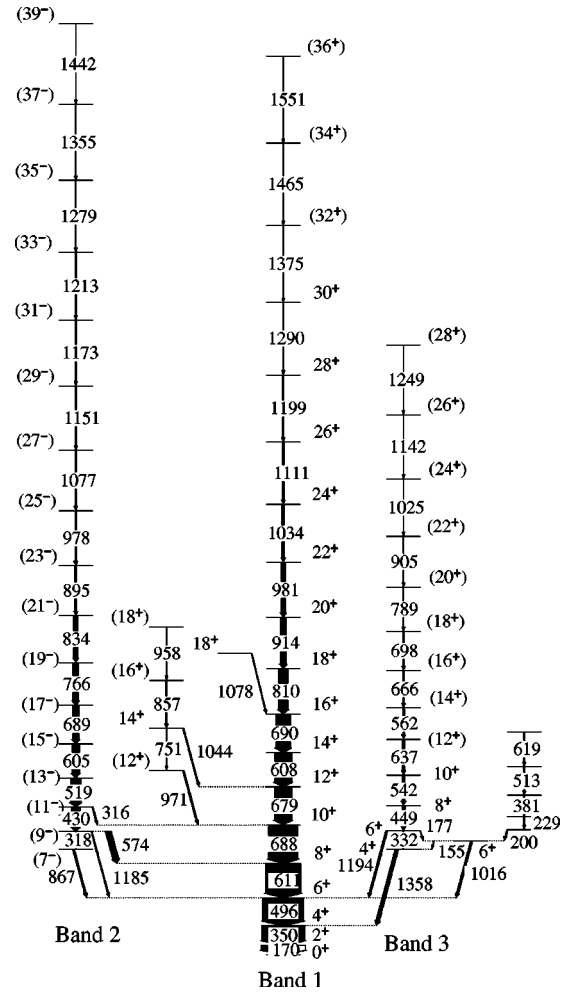

FIG. 1. Partial level scheme for ^{126}Ce deduced from the present work.

band up to the 1290-keV γ ray. Band members are marked with triangles; the two peaks marked with open triangles are near doublets within the band (608/611 keV and 688/690 keV). The inset shows the high-energy portion of the spectrum obtained by setting double gates of the form $(A \times B)$ where A is the list of γ rays with energies (170, 350, 496, 611, 688, 679, 607, 810, 914, 981, 1034 keV) and list B contains the γ rays with energies (1111, 1199, 1290, 1375, 1465 keV). Figure 2(b) shows a background-subtracted, double-gated spectrum obtained by setting gates on clean combinations of pairs of transitions in band 2 and projecting the 1D spectrum out of the particle-gated cube. Transitions in band 2 are marked with filled diamonds. The peaks marked with filled triangles represent transitions in the ground-state band fed by band 2. The inset shows the high-energy region of the same spectrum. Figure 2(c) shows a double-gated spectrum of band 3. All γ rays identified in band 3 were used to create this spectrum. Transitions in band 3 are marked with open diamonds. As for Fig. 2(b), transitions in the ground-state band fed by band 3 are marked with filled triangles. Linking transitions are marked with circles. The inset shows the high-energy region of the same spectrum.

TABLE I. Energies, intensities, and DCO ratios of transitions assigned to ^{126}Ce.

E_γ [a] (keV)	I_γ [b]	$I_i^\pi \to I_f^\pi$	R_{DCO} [c]	$M\lambda$
154.5	1.2(8)	$6^+\to4^+$		$(E2)$ [d]
169.7	79.0(1)	$2^+\to0^+$	0.808(10)	$E2$
177.2	1.8(8)	$6^+\to6^+$	0.4(2)	$M1/E2$ [e]
200.0	2.5(8)			
228.7	1.4(8)			
316.2	2.9(6)	$(11^-)\to10^+$	0.44(12)	$(E1)$
317.8	3.2(4)	$(9^-)\to(7^-)$	1.05(7)	$E2$
331.7	2.2(9)	$6^+\to4^+$	0.99(8)	$E2$
349.7	100.0	$4^+\to2^+$	0.882(9)	$E2$
381.0	1.2(9)			
429.7	19.5(1.6)	$(11^-)\to(9^-)$	1.06(8)	$E2$
449.4	6.4(6)	$8^+\to6^+$	0.93(4)	$E2$
496.2	96.0(4.0)	$6^+\to4^+$	1.073(18)	$E2$
513.2	2.0(9)			
519.3	22.4(1.9)	$(13^-)\to(11^-)$	1.14(5)	$E2$
541.9	3.6(3)	$10^+\to8^+$	0.99(4)	$E2$
562.1	3.4(3)	$14^+\to12^+$	1.07(12)	$E2$
573.8	12.3(1.2)	$(9^-)\to8^+$	0.64(3)	$(E1)$
604.5	18.1(1.7)	$(15^-)\to(13^-)$	1.01(8)	$E2$
607.6	36.3(2.0)	$14^+\to12^+$	0.97(6)	$E2$
611.0	70.2(3.0)	$8^+\to6^+$	1.07(5)	$E2$
619.4	1.8(9)			
637.1	3.5(8)	$(12^+)\to10^+$		$(E2)$
666.3	2.9(8)	$(16^+\to14^+)$		$(E2)$
678.5	36.2(2.9)	$12^+\to10^+$	0.99(2)	$E2$
687.5	54.7(4.6)	$10^+\to8^+$	1.02(5)	$E2$
689.4	14.9(1.5)	$(17^-)\to(15^-)$	1.3(3)	$E2$
689.6	22.1(2.0)	$16^+\to14^+$	1.12(17)	$E2$
698.2	2.2(9)	$(18^+\to16^+)$		$(E2)$
751.4	1.7(8)	$14^+\to(12^+)$		$(E2)$
765.8	14.1(7)	$(19^-)\to(17^-)$	1.03(8)	$E2$
789.4	1.9(6)	$(20^+\to18^+)$		$(E2)$
810.4	19.0(1.7)	$18^+\to16^+$	0.96(4)	$E2$
833.5	8.7(9)	$(21^-)\to(19^-)$	0.95(10)	$E2$
856.7	3.4(9)	$(16^+)\to14^+$		$(E2)$
867.1	3.5(1.0)	$(7^-)\to6^+$	0.65(7)	$(E1)$
895.4	3.9(5)	$(23^-)\to(21^-)$	0.91(14)	$E2$
904.8	1.3(9)	$(22^+\to20^+)$		$(E2)$
913.9	13.9(1)	$20^+\to18^+$	1.0(2)	$E2$
958.2	1.5(5)	$(18^+\to16^+)$		
970.9	2.5(4)	$(12^+)\to10^+$		$(E2)$
978.2	3.3(6)	$(25^-)\to(23^-)$	1.2(2)	$E2$
981.3	10.0(1.1)	$22^+\to20^+$	1.0(2)	$E2$
1016.0	5.1(5)	$6^+\to6^+$	0.6(2)	$M1/E2$
1025.4	1.0(9)	$(24^+\to22^+)$		$(E2)$
1034.4	6.9(9)	$24^+\to22^+$	1.1(3)	$E2$
1043.7	3.6(6)	$14^+\to12^+$	1.2(3)	$E2$
1076.6	1.5(5)	$(27^-)\to(25^-)$	1.2(3)	$E2$
1078.4	2.5(3)	$18^+\to16^+$	1.2(4)	$E2$
1110.6	3.8(5)	$26^+\to24^+$	1.1(3)	$E2$
1142.4	0.6(2)	$(26^+\to24^+)$		$(E2)$
1150.6	1.1(3)	$(29^-)\to27^-$		$(E2)$
1172.7	0.7(2)	$(31^-\to29^-)$		$(E2)$
1185.0	1.3(4)	$(9^-)\to6^+$	1.6(3)	$E3$
1193.8	3.6(3)	$6^+\to6^+$	1.3(4)	$E2$
1198.7	2.1(4)	$28^+\to26^+$	1.0(3)	$E2$
1213.0	0.7(2)	$(33^-\to31^-)$		$(E2)$
1249.0	0.3(2)	$(28^+\to26^+)$		$(E2)$
1278.7	0.6(2)	$(35^-\to33^-)$		$(E2)$
1289.6	1.6(7)	$30^+\to28^+$	1.0(3)	$E2$
1355.3	0.4(2)	$(37^-\to35^-)$		$(E2)$
1358.1	4.5(5)	$4^+\to4^+$	1.1(3)	$E2$
1375.0	1.1(8)	$(32^+\to30^+)$		$(E2)$
1442.0	0.20(12)	$(39^-\to37^-)$		$(E2)$
1464.8	0.5(2)	$(34^+\to32^+)$		$(E2)$
1550.7	0.29(14)	$(36^+\to34^+)$		$(E2)$

TABLE I. (*Continued*).

[a]Energies are accurate to ±0.2 keV for the strongest transitions (i.e., those carrying $\geq10\%$ of the intensity of the ^{126}Ce channel), with the uncertainty increasing to ±2.0 keV for the weakest transitions.

[b]The intensities given here have been obtained from the ungated RADWARE cube. Corrections have been made for detector efficiency.

[c]Values of R_{DCO} have been measured from four matrices, all four of which were gated on the detection of one or two protons and zero α particles. Where possible, measurements were performed in a matrix created with no γ-ray gates; additional measurements were made in matrices gated by transitions from band 2, band 3, and the lower portion of band 1.

[d]Assignment of $E2$ nature made on the basis of decay paths to and from this level involving other levels of fixed spin.

[e]Assignment of $M1$ made on the basis of intensity conservation considerations and internal conversion.

The spins and parities of the levels in Fig. 1 are based on the value of the ratio R_{DCO} measured for deexciting γ rays (see Table I). In some cases, these assignments are made or confirmed by other decay paths and intensity balances implying large internal conversion. For example, the 6^+ level at 2.032 MeV is assigned as such because of the decay from the 6^+ level in band 3. This occurs via a 177-keV transition; in order for intensity balances to be satisfied, internal conversion must be significant and thus the 177-keV γ ray feeding this level is required to be of $M1$ nature. If this transition were a stretched dipole, this would give a spin assignment of 5^+. However, this level itself decays directly into the 6^+ level in the ground-state band via a transition of 1016 keV that has a measured DCO ratio of 0.6(2). Following a heavy-ion reaction such as that used here, it is unlikely that ''up-hill'' transitions (going from I to $I+1$) will be observed. Thus we assign both the 177- and 1016-keV transitions as unstretched, mixed $M1/E2$ transitions. This in turn leads to the necessary assumption that the 155-keV transition carrying intensity from the state at 2.032 MeV into the lowest level of band 3 is a stretched $E2$.

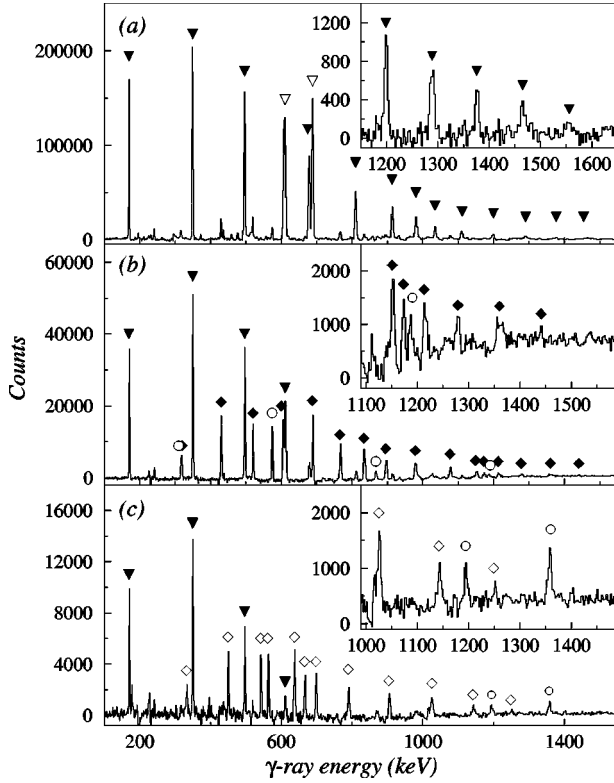In their work, Morek *et al.* assigned band 2 as being of

FIG. 2. (a) Triple-gated coincidence spectrum showing band 1 in ^{126}Ce. The filled triangles mark peaks corresponding to band members; the open triangles mark near doublets (at 608/611 keV and 688/690 keV). (b) Double-gated spectrum showing band 2 in ^{126}Ce. Band members are marked with filled diamonds, transitions in band 1 fed by band 2 are marked with filled triangles, and linking transitions are marked with open circles. (c) Double-gated spectrum showing band 3 in ^{126}Ce. Band members are marked with open diamonds; symbols marking other peaks are as for (b). The insets show the high-energy portion of each band.

negative parity. The DCO ratios obtained in the current work strongly support the assertion that the 867-, 574-, and 316-keV transitions connecting levels in band 2 and band 1 are of stretched dipole character. The low values of these ratios [0.65(7), 0.64(3), and 0.44(12), respectively] indicate a pure dipole nature, which is usually taken to indicate electric, rather than magnetic, character as $M1$ transitions are often admixed with $E2$ contributions. In addition, the systematics of neighboring Ce and Ba isotopes suggest that the first excited structure should be based on a negative parity configuration. There is no clear reason why ^{126}Ce should depart from systematic behavior observed to hold true for the even more neutron-deficient ^{124}Ce [16]. Thus it is tempting to retain the spin and parity assignment of the earlier work [6]. However, the observation of the 1185-keV transition connecting the level assigned as having $I^{\pi}=9^{-}$ to the 6^{+} level in band 1 casts some doubt on this assertion (see Sec. V B). For this reason, the spins and parities of the levels in band 2 are given in parentheses in Fig. 1 and Table I.

It should be noted that the ordering of the 542-, 637-, 562-, and 666-keV γ rays in band 3 is somewhat ambiguous. The transitions are in the plateau region of the band's inten-

sity pattern; in addition, some degree of contamination is brought into the spectrum from other nuclei. However, after careful analysis of the intensities, the sequence given here appears to be the most probable. The proposed order is also supported by consideration of the moment of inertia produced by the various possible orders—see below and Sec. V C.

In addition to the extension of the rotational bands, several other levels have been identified. In particular, the structure that decays into the 6^{+} level of the ground-state band via a 1016-keV transition has been extended. Cross-talk has been observed between the lowest levels of band 3 and the lowest level of this cascade, implying that there may be some underlying similarity between the two structures. However, the low intensity with which these levels are populated has precluded any definitive assignments of spin and parity.

The following discussion will concentrate on the three rotational bands (1, 2, and 3). To compare the behavior of the rotational bands with the predictions of standard and extended CSM calculations, one extracts the aligned angular momentum (I_x), experimental alignment (i_x) and dynamic moment of inertia ($\mathfrak{J}^{(2)}$) from the data using the following expressions:

$$I_x = [(I+1/2)^2 - K^2]^{1/2}; \tag{2}$$

$$i_x = I_x - I_x^{ref}; \tag{3}$$

where the reference value representing collective rotation (I_x^{ref}) is given by

$$I_x^{ref}(\omega) = (J_0 + \omega^2 J_1)\omega; \tag{4}$$

and

$$\mathfrak{J}^{(2)} \approx \frac{4\hbar^2}{\Delta E_{\gamma}}. \tag{5}$$

The Harris parameters J_0, J_1 most commonly used in this mass region are $J_0 = 17.0\hbar$ MeV^{-1} and $J_1 = 25.8\hbar^2$ MeV^{-3}. These values were originally obtained by fitting transitions above the first band crossing in the yrast structure of ^{130}Ce [17], and have been found to be appropriate for most of the structures observed in neighboring isotopes.

Figure 3(a) shows the alignment i_x extracted from the data for bands 1, 2, and 3. A value of $K=1$ has been assumed for band 2. [A particle-hole excitation from an $h_{11/2}$ orbital into the positive parity $g_{7/2}$ orbital would give rise to a structure with either $K=1$ or 2 (see Sec. V B).] Band 3 is assumed to have $K=0$. The spin of the lowest observed level in band 3 is $I^{\pi}=4^{+}$; however, the use of $K=0$ or $K=2$ is more appropriate in light of the discussion below (see Sec. V C), in which it is suggested that this structure may be based upon a γ-vibrational state. Figure 3(b) shows the dynamic moment of inertia $\mathfrak{J}^{(2)}$ for each band. In both figures, data for band 1 (the ground-state band) are shown with filled triangles, data for band 2 with filled diamonds and for band 3 with open diamonds.
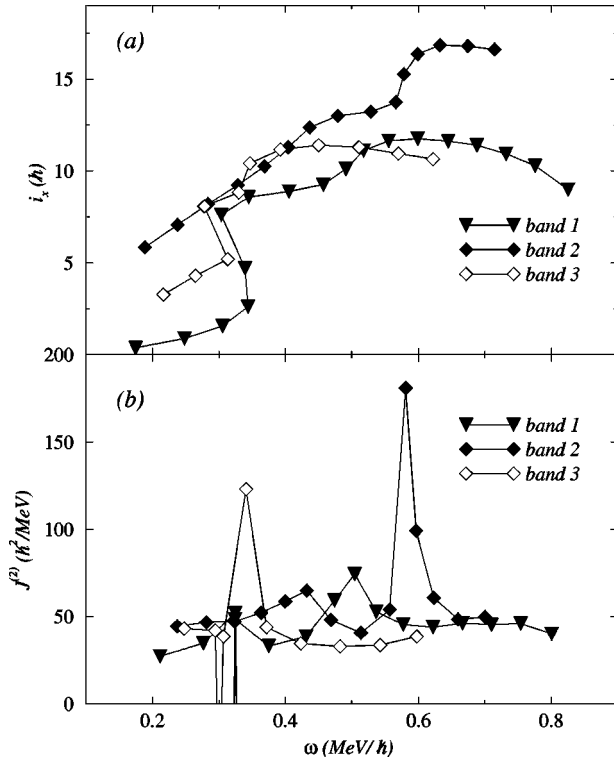
FIG. 3. (a) Alignment i_x as a function of rotational frequency for bands 1, 2, and 3 in ^{126}Ce. See text for details of the parameters used. (b) Dynamic moments of inertia $\mathfrak{J}^{(2)}$ for the three bands.

V. DISCUSSION

The results of standard CSM calculations for ^{126}Ce are shown in Fig. 4. The calculations have been performed using a triaxial Woods-Saxon potential [18,19] with deformation parameters $\beta_2 = 0.28$, $\beta_4 = 0.014$, and $\gamma = 0°$. The pairing strength is calculated at $\omega = 0$ MeV/$\hbar$ and decreases with increasing rotational frequency so that it has 50% of its initial value at $\omega = 0.7$ MeV/$\hbar$ [20]. Quasiproton levels are shown in Fig. 4(a) and the results for quasineutrons in Fig. 4(b).

The calculations for protons indicate that there are two pairs of negative-parity levels (originating from the $h_{11/2}$ [541]3/2$^-$ and [550]1/2$^-$ orbitals) lying close to the Fermi surface. These levels are labeled e, f, g, and h. The positive-parity orbitals in this mass region generally originate from the proton $g_{7/2}$ and $d_{5/2}$ shells; in the case of ^{126}Ce, the calculations show (for the deformations parameters above) that the lowest available positive-parity states (a,b quasiproton levels) are predominantly $g_{7/2}$ hole states (all these states have strong admixtures of other $d_{5/2}$, $g_{7/2}$ levels in the wave functions). The next available positive-parity excitation (c,d) appears to be another holelike state, this time based on a $g_{9/2}$ extruder orbital.

The calculations for neutrons show that the lowest quasiparticle states (E,F) are again negative-parity $h_{11/2}$ intruder states, this time a pair of near-degenerate signature partners originating from the ν[523]7/2$^-$ orbital. The quasineutron G,H excitations are based on the signatures of another $h_{11/2}$ pair (the [532]5/2$^-$ levels). The first positive-parity states
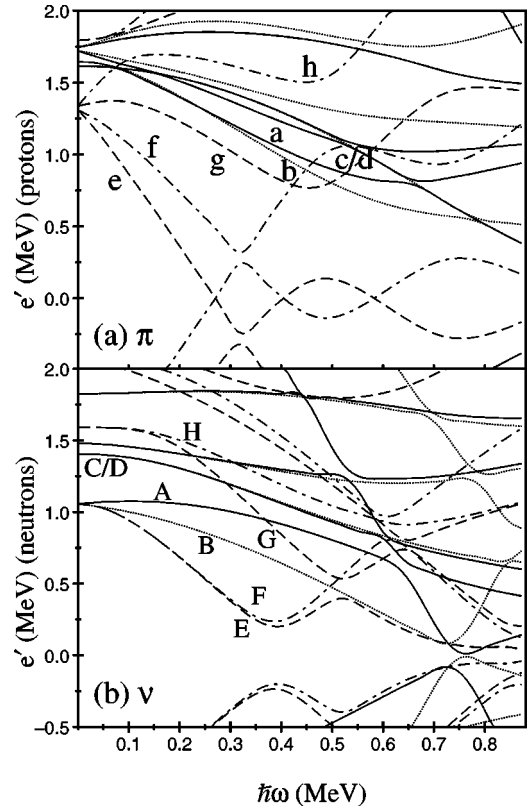

FIG. 4. Quasiparticle diagrams for ^{126}Ce obtained using standard cranked shell model calculations, showing (a) quasiproton and (b) quasineutron states. The parity and signature of the states is represented as follows: $(\pi,\alpha) = +,0$ states are shown with solid lines, $(\pi,\alpha) = +,1$ states are shown with dotted lines, $(\pi,\alpha) = -,0$ states are shown with dashed lines, and $(\pi,\alpha) = -,1$ are shown with dot-dashed lines. The asymptotic Nilsson numbers associated with the labels of the states can be found in Table II.

(A,B) should be particle-like excitations based on the [411]1/2$^+$ ($d_{3/2}$) orbitals. Other orbitals that may contribute to yrast and near-yrast structures are associated with the $d_{5/2}$ and $g_{7/2}$ subshells.

The various quasiparticle alignment frequencies predicted by these calculations are summarized in Table II.

It should be noted that isotopes in this region of the nuclear chart are often found to be fairly soft with respect to γ deformation. Total Routhian surface (TRS) calculations for ^{126}Ce reveal the presence of a stable but γ-soft minimum centered at $\beta_2 = 0.28$, $\gamma = 0°$ over a large spin range. Figure 5 shows an example of the results of these calculations obtained for the quasiparticle vacuum at $\omega = 0.0$ MeV/$\hbar$. The basic shape of the minimum remains unchanged up to about spin $I \approx 30\hbar$, where it begins to split into three separate minima with well-defined γ values. Although the occupation of $h_{11/2}$ orbitals tends to stabilize the deformation in terms of β_2, the softness with respect to γ is retained for several of the excited configurations. Low-lying γ-vibrational bands have been observed in some Ba and Xe isotopes [21–25]; on the basis of the results of the TRS calculations, one might expect to observe similar structures in the nearby Ce isotopes.

TABLE II. Summary of the quasiparticle levels close to the Fermi surface of ^{126}Ce at a deformation of $\beta_2 = 0.28$, $\gamma = 0°$. Alignment frequencies predicted by the standard cranked shell model calculations (shown in Fig. 4) are also given.

	Subshell	Nilsson configuration $[Nn_z\Lambda]\Omega^\pi$	Label $\alpha = +1/2$	$\alpha = -1/2$
Protons	$g_{7/2}$	$[422]3/2^+$	a	b
	$g_{9/2}$	$[404]9/2^+$	c	d
	$h_{11/2}$	$[541]3/2^-$	f	e
	$h_{11/2}$	$[550]1/2^-$	h	g
Neutrons	$d_{3/2}$	$[411]1/2^+$	A	B
	$d_{5/2}, g_{7/2}$	$[402]5/2^+$	C	D
	$h_{11/2}$	$[523]7/2^-$	F	E
	$h_{11/2}$	$[532]5/2^-$	H	G
Aligning quasiparticles		Frequency (MeV/$\hbar$)	Alignment gain ($\hbar$)	
EF		0.32	9	
FG		0.48	$5-6$	
EH		0.50	6	
AC		0.67	1	
ef		0.40	6	
fg		0.52	6	

A. Band 1

In their work, Morek *et al.* [6] observed band 1 through its first backbend (occurring at spin $I \approx 10\hbar$) up to a spin of $I = 20\hbar$. The present study confirms their findings and extends this band by eight transitions to a maximum observed spin of $I = 36\hbar$. The first crossing occurs at rotational frequency $\omega \approx 0.33$ MeV/$\hbar$ and results in an alignment gain of

FIG. 5. An example of the results of total Routhian surface calculations for ^{126}Ce. The calculations shown were performed for the quasiparticle vacuum at rotational frequency $\hbar\omega = 0.0$ MeV. The position and shape of the minimum (which is centered around $\beta_2 = 0.28$, $\gamma = 0°$) remain relatively unchanged over a large-spin range (up to around $I \approx 30\hbar$). See text for further details.

$\approx 10\hbar$. As Morek *et al.* suggested, this crossing can most easily be understood as the alignment of a pair of $h_{11/2}$ protons. The standard CSM calculations predict that the first $h_{11/2}$ protons (ef) will align at $\omega \approx 0.32$ MeV/$\hbar$ (see Fig. 4). Thus it is reasonable to suggest that band 1 corresponds to the quasiparticle vacuum at low frequencies and that, above the first backbend, it is based upon the πef configuration.
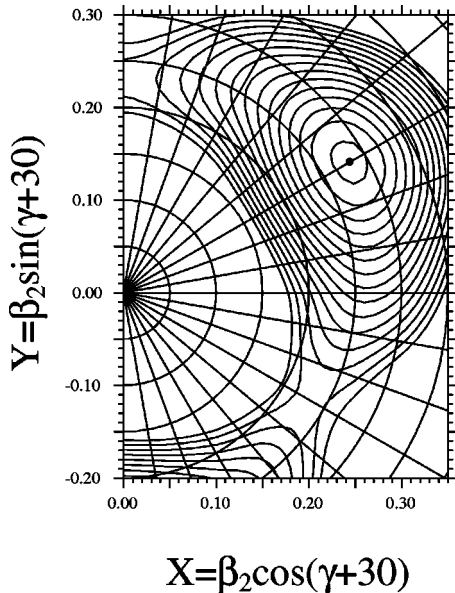
The additional transitions observed in this data allow the clear identification of a second, gradual alignment occurring around $\omega \approx 0.5$ MeV/$\hbar$. Figure 6(a) shows the alignment i_x of this band as a function of rotational frequency. The ground-state bands of neighboring even-even isotopes are included for comparison. It is immediately obvious that ^{126}Ce undergoes some interaction giving rise to an alignment gain at $\omega \approx 0.5$ MeV/$\hbar$, and that this interaction does not occur in the ground-state bands of the other Ce isotopes. According to the calculations, one should expect three possible alignments occurring around $\omega \approx 0.45$ MeV/$\hbar$ (see Table II); however, both the eh and fg quasiproton alignments would be blocked in the case of the ef band. This leaves the quasineutron EF crossing, which is predicted to occur at the somewhat lower frequency of $\omega \approx 0.4$ MeV/$\hbar$. The failure of the calculations to reproduce the crossing frequency correctly is typical of experimental observation in this mass region. It appears that some modification of the calculations is necessary.

Recent work by Parry *et al.* [2] showed that extended CSM [4] calculations (in which both pairing and deformation are determined self-consistently) provide a good framework in which to describe the behavior of these neutron-deficient nuclei. There, it was shown that the rise in the $\mathfrak{I}^{(2)}$ of the yrast sequence in ^{127}Pr (and also in ^{131}Pm) is due predominantly to the alignment of a pair of $h_{11/2}$ neutrons, although there is some contribution from the $h_{11/2}$ protons too. The
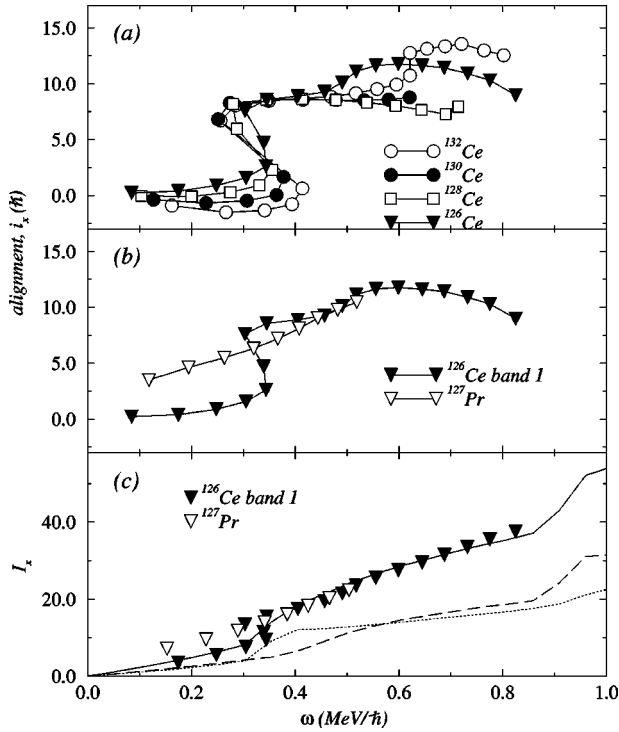
FIG. 6. (a) Alignment i_x as a function of rotational frequency for the yrast structures in $^{126-132}$Ce. (b) Alignment of the yrast structures in ^{126}Ce and ^{127}Pr. (c) Aligned angular momentum I_x for band 1 in ^{126}Ce, compared to the results of the extended CSM calculations. The total I_x predicted by the calculations is shown by the solid line; the contribution from protons and neutrons are shown by dotted and dashed lines, respectively.

calculations reproduce the frequency range over which the alignment is observed, as well as the interaction strength. An extension of the study to heavier, odd-A Pr and Pm isotopes indicates that the frequency at which the $h_{11/2}$ neutrons align increases with increasing neutron number. Thus, it is only for the lighter isotopes that the neutron component around $\omega \approx 0.5$ MeV/$\hbar$ is substantial. Figure 6(b) shows the quantity i_x extracted for the ground-state bands in both ^{126}Ce and ^{127}Pr. The band in ^{127}Pr has a larger initial alignment (as one would expect with the extra proton occupying an $h_{11/2}$ orbital), but the increase in i_x occurs at almost the same frequency and with the same character as the second alignment in the band in ^{126}Ce. Extended TRS calculations performed for ^{126}Ce confirm that (as the standard calculations shown in Fig. 5 suggest) the ground-state band is built on the quasiparticle vacuum with a deformation of $\beta_2 \approx 0.28$, $\gamma \approx 0°$. The alignment of a pair of $h_{11/2}$ protons (blocked in the odd-Z neighbor) is predicted to occur over the frequency range $\omega \approx 0.3-0.4$ MeV/$\hbar$. A second interaction (the alignment of a pair of $h_{11/2}$ quasineutrons) is predicted to occur between $\omega \approx 0.4$ and $\omega \approx 0.5$ MeV/$\hbar$. Figure 6(c) shows the total alignment I_x predicted for this band compared to the experimental data for band 1. The separate contributions from protons and neutrons are indicated by dotted and dashed lines, respectively. A second neutron alignment is predicted at $\omega \approx 0.9$ MeV/$\hbar$, coinciding with a smaller effect in the proton alignment. The present data do not extend to such high rotational

frequency, but a future extension of the band would provide excellent confirmation of the mechanisms underpinning the alignment characteristics. However, on the basis of these results it is possible to assign configurations as follows: for $I = 0-10\hbar$, band 1 is built upon the quasiparticle vacuum; for $I = 10-20\hbar$, it corresponds to the πef configuration; and for $I = 20\hbar$ to the experimentally observed limit, it corresponds to the $\pi ef \nu EF$ configuration.

B. Band 2

Morek *et al.* suggested that band 2 is a negative-parity band with $K = 5$. The DCO ratios obtained from the current data partially support the assumption of negative parity; however, the observation of a transition (of energy 1185 keV) linking band 2 to band 1 may cast some doubt on this assignment. The results of the CSM calculations (see below) also suggest that the band may not be based on a configuration with $K = 5$.

The improved statistics obtained with the GAMMAS-PHERE array allow a more accurate determination of the DCO ratios of the 316-, 574-, and 867-keV transitions linking levels in band 2 with levels in the ground-state band; the measured values (see Sec. IV) suggest a stretched dipole character for these γ rays, which in turn suggests that band 2 is most likely to have negative parity and that the spin of the lowest observed level is $7\hbar$. This fits with the systematics of heavier Ce nuclei, in which a negative-parity band with $K = 5$ is observed to be one of the lowest excitations. Indeed, recent work [16] suggests that this systematic behavior extends to the more neutron-deficient ^{124}Ce. The even-even Ba nuclei, which in general exhibit similar behavior to their Ce isotones, also conform to this pattern. However, an additional transition of 1185 keV has been observed in the present data, linking the state in band 2 fed by the 430-keV transition to the 6^+ level in band 1. The low intensity of this transition precludes an accurate measurement of the DCO ratio, but, if one accepts that the other connecting transitions are electric dipoles, then this transition must be an $E3$. The presence of an experimentally observable $E3$ would indicate some degree of octupole collectivity, and thus the question of whether this is likely must be given some consideration. The ''magic numbers'' for octupole deformation have been given by Nazarewicz *et al.* [26] as 34, 56, 88, and 134. Strong evidence for static octupole deformations has been observed in nuclei with $Z \approx 56$, $N \approx 88$ (for example, ^{144}Ba [27]); indeed, Cottle [28] suggested that these magic numbers would be modified and that a region of static octupole deformation should exist in nuclei close to ^{126}Ba. Subsequent experimental evidence [29] did not support this proposal; however, the possibility of *collective* octupole effects subsisting in these nuclei remains an interesting and unanswered question. Thus it is not unreasonable to suggest that octupole degrees of freedom may play a part in determining the structure of the Ce isotopes ($Z = 58$).

A good indication of the presence of a transition dipole moment arising from an octupole vibrational state can be obtained from the experimental $E1$ strength, which is enhanced by the charge asymmetry of the vibration. An esti-

mate of the $B(E1)$ strengths for the 316-keV and 574-keV transitions deexciting the levels assigned as 9^- and 11^- in band 2 has been obtained from the data using the following expressions:

$$\frac{B(E1)}{B(E2)} = 0.77 \times 10^{-6} \frac{E_\gamma^5(E2)}{E_\gamma^3(E1)} \frac{I_\gamma(E1)}{I_\gamma(E2)} \quad (6)$$

and

$$B(E2) = \frac{5}{16\pi} Q_0^2 \langle IK20|I-2K\rangle^2 (e\,\text{b})^2. \quad (7)$$

If one inspects the results of the CSM calculations (Fig. 4 and Table II), it appears that the lowest-lying negative parity excitations will be built on a particle-hole excitation from an $h_{11/2}$ orbital (giving $K=1/2$) to a $g_{7/2}$ orbital (giving $K=3/2$). The DCO ratios obtained for the transitions linking band 2 to band 1 suggest a spin difference $\Delta I=1$, which implies that this band has odd spins. Thus it appears, if the CSM calculations are correct, that band 2 has $K=1$ rather than $K=5$. Hence, in evaluating Eq. (7), a value of $K=1$ has been used, together with a value of $Q_0=4.5\ e$ b (corresponding to an axially symmetric shape with $\beta_2=0.28$). The experimental values of $B(E1)$ obtained in this way are $B(E1)_{9^-}=2.0(5)\times 10^{-4}$ W.u. and $B(E1)_{11^-}=1.7(4)\times 10^{-4}$ W.u. (the errors assume no uncertainty in the values of I, K, and Q_0). $E1$ strengths of this magnitude are indicative of the presence of octupole correlations (in this case, a vibrational state is more likely than a static octupole deformation) and thus the presence of an experimentally observable $E3$ transition is not unlikely. An estimate of the $E3$ strength associated with the 1185-keV transition can similarly be extracted from the data; using the same values of I, K, and Q_0 this is obtained as $B(E3)_{9^-}=4.7(1.9)\times 10^3$ W.u. This is somewhat higher than might be expected. As before, the uncertainty quoted for this value does not include the possible contribution from the value of $B(E2)$ employed in the calculation. Assuming a value of $K=2$ would result in a slight reduction of the $E3$ strength; however, if the standard CSM calculations are not accurate in this region (as is indicated by the results concerning band 1), it is possible that in fact a different configuration might be possible and that the band, like its counterparts in the heavier Ce nuclei, may have $K=5$. This would result in the $B(E3)$ being approximately halved. A further significant decrease can be achieved by assuming a smaller quadrupole moment. In order to reduce the value obtained for the $B(E3)$ by a further factor of 2, Q_0 would need to be as low as 3.2 e b. One might expect the axial deformation of the nucleus to be reduced by the presence of an octupole surface vibration and hence this may not be an unreasonable assumption. Thus, with these changes to the values of K and Q_0 employed in the equations, an $E3$ strength of $1.1(0.5)\times 10^3$ W.u. can be arrived at. Although this value is still somewhat large, it is not impossible that such a strong transition might occur.

Of course, the above series of assumptions cannot be made with confidence, and alternative possibilities must be considered. One scenario could be that the spins of the levels in band 2 are each reduced by $2\hbar$. This would result in an $E1$ nature for the 1185-keV transition, which would then be connecting a level of spin $I=7$ in band 2 with the $I=6$ level in the ground-state band. Such an adjustment would imply that the 867-, 574-, and 316-keV γ rays are ''up-hill'' transitions, carrying intensity from levels of spin I to levels of spin $I+1$. As was argued in relation to the decay-out of band 3, however, such transitions are unlikely to be observed following heavy-ion fusion-evaporation reactions. A third possible explanation would be that band 2 is in fact of positive parity and that the spin of the lowest level is 5^+. This would result in the 1185-keV transition being of $E2$ nature, while the three other transitions carrying intensity to band 1 would then be magnetic, rather than electric, dipoles. This would imply a serious departure from the systematics of the lowest excited bands observed in other even-even Ce and Ba isotopes. Although the discussion of band 1 above indicates that standard CSM calculations are not adequate in describing the behavior of nuclei in this mass region, there is no evidence to suggest that ^{126}Ce should be expected to deviate from the otherwise consistent behavior of the neighboring isotopes. In addition, the DCO ratios indicate pure stretched dipoles for the 316-, 574-, and 867-keV transitions, whereas one would expect a significant degree of mixing with an $E2$ component if the transitions were magnetic dipoles.

Altogether, none of the above options for assigning spins and parity to band 2 is quite satisfactory. The remainder of the discussion assumes that the spins assigned to the levels shown in Fig. 1 are correct, but it should be borne in mind that a large amount of uncertainty remains.

An inspection of Fig. 3(a) reveals that band 2 undergoes a smooth gain in alignment (from 5 to $13\hbar$) up to $\omega=0.48$ MeV/$\hbar$, followed by a sharp increase at $\omega=0.57$ MeV/$\hbar$ taking it to a maximum value of $\approx 17\hbar$. According to the standard CSM calculations, the lowest available negative-parity state should be based on the be quasiproton configuration. Assuming the assigned spins are correct, the initial alignment of $5\hbar$ for band 2 supports this assignment (the occupied $h_{11/2}$ orbital should be expected to contribute this amount), as does the lack of evidence for the πef alignment, which would be blocked. The $\mathfrak{J}^{(2)}$ moment of inertia [see Fig. 3(b)] indicates a strong interaction occurring around $\omega=0.45$ MeV/$\hbar$; the general shape of this interaction is similar to that observed at slightly higher frequency in band 1. The latter has been explained as the alignment of the EF neutrons in the above discussion. The frequency at which this crossing is predicted to occur is very sensitive to the deformation of the nucleus; a reduction in quadrupole deformation as compared to the ground-state band could be responsible for the observed difference, as could a change in the triaxiality parameter γ. If this change in crossing frequency does indeed indicate a reduced β_2, this lends some support to the arguments given above suggesting that the $B(E3)$ can be lowered. Additionally, the effects of an octupole vibrational component might also alter the predicted crossing frequencies. Thus, it seems probable that

band 2 is initially based on the πbe two-quasiproton excitation, gaining the EF quasineutron pair around spin $I=23\hbar$. However, the most dramatic feature of the band is the rapid increase in i_x observed at $\omega=0.57$ MeV/$\hbar$. The standard calculations predict no alignments around this frequency, with the closest being the neutron FG alignment at $\omega=0.52$ MeV/$\hbar$ (which would in any case be blocked if the earlier rise is interpreted as the νEF pair aligning) and the πeh quasiproton alignment (which would again be blocked if this band is based on the πbe configuration). Extended calculations have not been performed for the excited states, but one can conjecture that this weak interaction, providing the nucleus with a further $4-5\hbar$ in aligned angular momentum, represents the alignment of the fg proton pair, predicted by the standard calculations to occur at rotational frequency $\omega=0.48$ MeV/$\hbar$. The strength of the interaction and the resulting increase in alignment are similar to what would be expected as this $h_{11/2}$ proton pair aligns with the rotation of the nuclear core. The difference between observed and predicted alignment frequencies is difficult to explain, particularly as the inadequacies of the standard calculations have generally only been apparent with respect to the behavior of the quasineutron levels in neighboring nuclei. However, if one discounts the Pauli-blocked band crossings, this seems to be the most likely remaining candidate.

In summary, it is possible that band 2 represents, at the lowest observed frequencies, the two quasiparticle πbe configuration. The slow aligning of the EF neutron pair is observed up to intermediate frequencies, suggesting that the band can be described as the $\pi be\nu EF$ configuration above spin $I=21\hbar$. The highest observed frequencies may represent the $\pi befg\nu EF$ configuration, in which four $h_{11/2}$ quasiprotons and two $h_{11/2}$ quasineutrons are aligned with the rotating core. However, it is not possible to confirm this assignment with the results of standard CSM calculations, which predict a much lower frequency for the second proton alignment. The difficulties encountered in explaining the features of this band highlight the inadequacy of the standard CSM in this mass region. In particular, the need to postulate different deformations points to a corresponding need for calculations in which the deformation is determined self-consistently. Experimentally, clearer data concerning the angular distributions associated with the transitions linking band 2 to band 1 must be obtained in order to define the spin and parity of the band. If it is found to be of positive parity, such a result would have serious implications for what has been thought to be the systematic behavior previously observed in the Ce/Ba region.

C. Band 3

The structure labeled band 3 in this work differs considerably from the third band observed by Morek *et al.* The reported 400-keV transition towards the bottom of the band has not been observed, an omission that considerably alters the alignment characteristics of the band. This band has been extended to spin $28\hbar$ and excitation energy 10.873 MeV, and is thought to be of positive parity. Two transitions (of energies 1358 and 1194 keV) have been observed in the data that link this band directly to the ground-state band. Although the DCO ratios obtained for these transitions are consistent with a stretched quadrupole character, it is in fact more likely that both decays are via unstretched transitions connecting states with the same spin and parity. If the transitions are assumed to take away two units of spin, then band 3 is close to yrast at lower spins and, indeed, becomes yrast around $I=22\hbar$. If one considers the weak intensity with which this band is populated (with respect to bands 1 and 2) it seems very unlikely that it is, in fact, yrast. Thus we are inclined to favor an assignment of $I^{\pi}=4^{+}$ to the lowest observed level.

As was noted above, the ordering of the γ rays between the 8^{+} and 16^{+} levels is somewhat ambiguous. The sequence given here appears to be the most likely, however, not only on the grounds of intensity considerations, but also in order to produce the most ''reasonable'' behavior in terms of the band's aligned angular momentum and dynamic moment of inertia. Both of these quantities, presented in Fig. 3, show evidence for the ef quasiproton alignment at a slightly lower frequency ($\omega=0.3$ MeV/$\hbar$) than in band 1. It is very difficult to explain the subsequent ''kick'' in the $\mathfrak{I}^{(2)}$ observed at $\omega=0.32$ MeV/$\hbar$, however any rearrangement of the γ rays leads to an even worse situation. For example, an alternative sequence of 449-, 542-, 562-, 637-, 666-keV γ rays leads to two separate interactions taking place at $\omega=0.24$ and 0.30 MeV/$\hbar$; the first alignment is then impossible to explain without altering the deformation and pairing parameters in the CSM calculations to unphysical values, while the second alignment has none of the features one would associate with the ef proton alignment. Thus, despite the ambiguity, one can be fairly confident that the proposed order is correct. The general characteristics of the band suggest a strong similarity with the structure of the ground-state band. It has a slightly larger initial alignment, but clearly undergoes the πef alignment, resulting in an increased i_x of $\approx 11.0\hbar$. Above $\omega\approx 0.3$ MeV/$\hbar$, there is no other evidence of any interaction taking place.

Inspection of the quasiparticle Routhians shown in Fig. 4 indicates that the lowest available positive-parity two-quasiparticle excitation would arise from a coupling of the $[541]3/2^{-}$ and $[550]1/2^{-}$ orbitals. However, the ef proton alignment, which is clearly visible in band 3, would be blocked for such a structure. Thus it is extremely unlikely that this band is based on this configuration. As was mentioned above, γ-vibrational structures have been observed in several neighboring Ba and Xe isotopes and TRS calculations suggest that ^{126}Ce may also support such vibrational modes. In their study of ^{126}Ba, Ward *et al.* [25] interpreted bands 1 and 2 of that nucleus as being the two signatures of a quasi-γ-vibrational band. These positive-parity bands were observed to decay directly to the ground state and to excited states within the ground-state band via a series of $E2$ and mixed $E2/M1$ transitions. The data revealed that this vibrational state underwent an alignment around $\omega=0.39$ MeV/$\hbar$, the same frequency at which the first $h_{11/2}$ quasiproton alignment takes place in the ground-state band. Above this alignment, the bands were interpreted as being based upon a γ vibration coupled to the aligned two-quasiparticle configuration of the S-band. By analogy, it is

possible to suggest that band 3 of ^{126}Ce represents the favored signature of a similar structure (a quasi-γ vibration of the vacuum configuration), and that above the crossing seen at $\omega \approx 0.3$ MeV/$\hbar$ it can be interpreted as a quasi-γ-S-band (i.e., γef in the notation used above). The decay of this band to the ground-state band via $E2$ transitions alone might indicate a more pure vibrational state than was observed in ^{126}Ba. However, if band 3 were indeed a γ-vibrational structure based on the vacuum configuration at low frequency and subsequently the two-quasiproton ef configuration above spin $I \approx 14\hbar$, then (by analogy with band 1) one might also expect to see evidence of the EF neutron alignment. In fact, above the initial interaction the dynamic moment of inertia of band 3 is remarkably smooth. It may be that the neutron alignment is altered by the presence of the γ vibrations; however the evidence is such that a γ-vibrational nature can only tentatively be assigned to this band.

VI. CONCLUSIONS

The use of the GAMMASPHERE array, in conjunction with the MICROBALL charged-particle detector, has allowed the expansion and clarification of the level scheme of the neutron-deficient nucleus ^{126}Ce. The three previously observed bands have been extended to higher spins and other structures identified. In all three cases, it has not been possible to provide adequate explanations of the characteristics of the bands using standard CSM calculations alone. The use of self-consistent, extended CSM calculations for the vacuum state have provided a clearer picture of the changes in structure undergone by band 1, which has been assigned the vacuum, πef and $\pi ef \nu EF$ configurations at low, intermediate and high spins. It seems most likely that, at the lowest frequencies, band 2 represents the lowest negative-parity configuration (the πbe quasiproton state). The first, strong interaction may be explained as the EF quasineutron alignment; the lower rotational frequency at which this occurs in band 2 may be due to a lower deformation. It has been suggested that the interaction observed at $\omega = 0.57$ MeV/$\hbar$ is due to the delayed alignment of the fg quasiproton pair; however, it is not possible to confirm this with the current data. In particular, the uncertainty concerning the assignment of parity to this band means that no firm statements can be made regarding the configurations responsible for the structure. Further experimental investigation concerning this matter is highly desirable, as the implications for the systematic interpretation of bands in Ce and Ba nuclei in this region are quite serious. Finally, whilst there is some evidence that band 3 may represent a γ-vibrational state coupled to the vacuum configuration at low spins and the ef quasiproton configuration at intermediate to high spins, no definite assignment can be made from the present experimental data.

[1] R. Wyss and W. Satula, Phys. Lett. B **351**, 393 (1995).

[2] C.M. Parry *et al.*, Phys. Rev. C **57**, 2215 (1998).

[3] S. Bouneau *et al.*, Phys. Rev. C **53**, R9 (1996).

[4] W. Satula and R. Wyss, Phys. Scr. **T56**, 159 (1995).

[5] E.S. Paul *et al.* (unpublished).

[6] T. Morek, K. Starosta, Ch. Droste, D. Fossan, G. Lane, J. Sears, J.F. Smith, and P. Vaska, Eur. Phys. J. A **3**, 99 (1998).

[7] I.Y. Lee, Nucl. Phys. **A520**, 641c (1990).

[8] C.N. Davids and J.D. Larson, Nucl. Instrum. Methods Phys. Res. B **40/41**, 1224 (1989).

[9] D.G. Sarantites, P.-F. Hua, M. Devlin, L.G. Sobotka, J. Elson, J.T. Hood, D.R. LaFosse, J.E. Sarantites, and M.R. Maier, Nucl. Instrum. Methods Phys. Res. A **381**, 418 (1996).

[10] D.C. Radford, Nucl. Instrum. Methods Phys. Res. A **361**, 297 (1995).

[11] B. Crowell, M.P. Carpenter, R.G. Henry, R.V.F. Janssens, T.L. Khoo, T. Lauritsen, and D. Nisius, Nucl. Instrum. Methods Phys. Res. A **355**, 575 (1995).

[12] W.T. Milner (private communication).

[13] M. Bergström (private communication).

[14] G. Palameta and J.C. Waddington, Nucl. Instrum. Methods Phys. Res. A **234**, 476 (1985).

[15] K.S. Krane, R.M. Steffen, and R.M. Wheeler, At. Data Nucl. Data Tables **11**, 351 (1973).

[16] J.F. Smith *et al.*, Phys. Rev. C (to be submitted).

[17] D.M. Todd, R. Aryaeinejad, D.J.G. Love, A.H. Nelson, P.J. Nolan, P.J. Smith, and P.J. Twin, J. Phys. G **10**, 1407 (1984).

[18] W. Nazarewicz, J. Dudek, R. Bengtsson, and I. Ragnarsson, Nucl. Phys. **A435**, 397 (1985).

[19] S. Cwiok, J. Dudek, W. Nazarewicz, W. Skalski, and T. Werner, Comput. Phys. Commun. **46**, 379 (1987).

[20] R. Wyss, J. Nyberg, A. Johnson, R. Bengtsson, and W. Nazarewicz, Phys. Lett. B **215**, 211 (1988).

[21] K. Schiffer, A. Dewald, A. Gelberg, R. Reinhardt, K.O. Zell, S. Xianfu, and P. von Brentano, Z. Phys. A **327**, 251 (1987).

[22] H. Wolters, K. Schiffer, A. Gelberg, A. Dewald, J. Eberth, R. Reinhardt, K.O. Zell, P. von Brentano, D. Alber, and H. Grawe, Z. Phys. A **328**, 15 (1987).

[23] C.B. Moon *et al.*, Nucl. Phys. **A510**, 173 (1990).

[24] S. Pilotte *et al.*, Nucl. Phys. **A514**, 545 (1990).

[25] D. Ward *et al.*, Nucl. Phys. **A529**, 315 (1991).

[26] W. Nazarewicz, P. Olanders, I. Ragnarsson, J. Dudek, G.A. Leander, P. Möller, and E. Ruchowska, Nucl. Phys. **A429**, 269 (1984).

[27] W.R. Phillips, I. Ahmad, H. Emling, R. Holzmann, R.V.F. Janssens, T.L. Khoo, and M.W. Drigert, Phys. Rev. Lett. **57**, 3257 (1986).

[28] P.D. Cottle, Z. Phys. A **338**, 281 (1991).

[29] P.D. Cottle, T. Glasmacher, J.L. Johnson, and K.W. Kemper, Phys. Rev. C **48**, 136 (1993).